scientific reports

Check for updates

OPEN

RORα fine-tunes the circadian control of hepatic triglyceride synthesis and gluconeogenesis

Chloé Monnier[1], Munkhzul Ganbold[1], Martine Auclair[1], Natacha Roblot[1], Andréas Barnabé Boutin[1], Paul Ketil Boutin[1], Bruno Fève[1,2] & Bénédicte Antoine[1]✉

Circadian rhythms play a fundamental role in hepatic metabolism, orchestrating lipid synthesis and glucose homeostasis. RORα, a nuclear receptor involved in circadian regulation, has been implicated in fine-tuning these metabolic processes. We previously showed a therapeutic potential of antagonizing RORα to reduce body fat in mice. Our current aim is to investigate the impact of the whole-body RORα deletion on hepatic lipid metabolism over a complete circadian cycle. Using RORα-knockout (staggerer) mice, this study reveals a time-dependent disruption in hepatic triglyceride synthesis, with reduced lipogenesis during the light-phase and altered transcriptional regulation of key metabolic genes, including Srebp1c and Insigs. Despite increased Srebp1c transcription at night, the anticipated rise in lipid synthesis was prevented by phase-shifted Insig expression, modulating precursor maturation. Moreover, core clock genes rhythmic expression was attenuated and phase-shifted for Reverbα. Pharmacological inhibition of RORα using an inverse agonist (SR3335) mirrored the metabolic effects observed in staggerer mice, further supporting the role of RORα as a crucial regulator of lipid and glucose homeostasis in mice fed a chow diet. These findings highlight the intricate interaction between the circadian clock and hepatic metabolism, situating RORα as a promising target to prevent metabolic disorders such as obesity and dyslipidemia.

Keywords Liver, Lipid synthesis, RORα, Circadian rhythms, Gluconeogenesis, Staggerer

A large body of experimental and clinical observations supports the strong relationship between metabolic processes and circadian clocks[1]. The molecular circadian clock machinery is composed of a master clock located in cells of the supra-chiasmatic nucleus (SCN). This master clock paces peripheral clocks throughout the body of mammalian species[2]. This ensures optimal coordination of active and rest phases, feeding and other anticipated and repetitive daily tasks, to peak expression of metabolism genes involved in those activities[1]. Some organs—including the liver- are not paced exclusively by the SCN master clock, but also by feeding[3].

The molecular circadian clock machinery includes 4 master genes that compose its core loop (*Clock, Bmal1, Per2* and *Cry1*), which is regulated by an additional feedback loop. The nuclear receptors RORs and Reverbs are involved in this feedback loop by binding to RORE sequences[4] on some target clock genes (*Clock*, *Bmal1*, *Cry1*), RORs being activators[5] and Reverbs repressors[6]. RORα, RORγ and Reverbα have been implicated in the regulation of glucose and lipid metabolism and in energy homeostasis[7]. The whole-body RORα-KO or RORγ-KO mouse models share similarities (hypoglycemia, hypotriglyceridemia)[8,9], while Reverbα-KO exhibit a trend towards an opposite phenotype[10]. Despite some redundancy between RORα and RORγ in target genes[11], they also have specific functions. Indeed, the stagerrer (sg/sg) mice, a spontaneous mutant RORα-KO, are characterized by slenderness and improved metabolic phenotype. Exhibiting lower plasma levels of triglycerides (TG), cholesterol, insulin and glucose[8,9,12], sg/sg mice resist to hypercaloric diet-induced dysfunctions, in spite of relatively higher food consumption[13]. They display reduced mass in fat depots,—with down-regulation in inflammatory gene expression[9,14], higher insulin sensitivity and lower fatty acid re-esterification via glyceroneogenesis[15]. This lean phenotype has been linked to the beiging of their white adipose depots that increases both thermogenesis and overall energy expenditure[16,17]. At the liver level, a lower rate of gluconeogenesis is observed[15], and a decreased TG content associated with a down-regulation of the genes involved in lipid synthesis is reported by most studies[8,9].

Considering the worldwide challenge in the prevention and management of metabolic diseases, the improved metabolic phenotype of the sg/sg mouse hints at the relevance of this model to identify new molecular

[1]UMR_S938, Centre de Recherche Saint-Antoine, IHU ICAN, Faculté de Médecine Site Saint-Antoine, Sorbonne Université-Inserm, 27 Rue Chaligny, 75012 Paris, France. [2]APHP, Department of Endocrinology and CRMR PRISIS, Saint-Antoine Hospital, Paris, France. ✉email: benedicte.antoine@inserm.fr

mechanisms underlying whole-body regulation of energy storage and utilization. There was an interest in designing therapies that could modulate RORα activity, and natural or chemical ligands were identified[18]. RORα agonist and inverse-agonists modulated physiological *PCK1*-dependent pathways in adipose tissue and liver[15,19]. First used as in vitro tools on isolated organs, such compounds regulate glyceroneogenesis in adipose tissue and gluconeogenesis in the liver[15]. We also showed that a selective RORα inverse-agonist (SR3335) was an inducer of fat browning[20], before being administrated in vivo in mice, where it was confirmed to increase adaptive thermogenesis and decrease fat mass[17]. This, combined with its hypoglycemic effect[19], made SR3335 an attractive compound to prevent obesity and related metabolic disorders[17]. Further emphasis was placed on identifying potential targets, modulated through dampening RORα signaling pathways in other organs, and particularly in the liver.

Indeed, whilst the whole-body RORα-KO model (sg/sg) presented reduced liver TG content compared to WT mice regardless of their food intake[8,9], this was not the case for liver-specific-RORα-KO (L-RORα-KO) mice on chow diet[21,22] or western diet[21]. This suggested that the hepatic lipid metabolism per se did not seem to be a major autonomous target of RORα. It also hinted that multiple organs contribute to the phenotype of sg/sg mice. Of note, the liver-specific depletion of both RORα and RORγ (L-RORαγ-KO) has been shown to display up-regulated expression of lipogenic genes during the night (active period) exclusively, with a trend to increased hepatic TG in the night on chow diet[23]. This highlighted autonomous metabolic role of RORs in the liver, dependent on the circadian rhythm. Unfortunately, most of the metabolic studies performed on sg/sg mice did not take into account circadian rhythms, with analysis only performed during the day, which is not adequate for exploring all metabolic pathways. This represents a major issue when investigating the role of RORα, a transcription factor that directly interacts with several major effectors of the core clock. Further work would help distinguish between autonomous and non-autonomous role of RORα in liver metabolism.

The aim of this study was to explore the lipid metabolism of the liver in the whole-body RORα-KO mice (sg/sg) over a full circadian cycle (*i.e.* throughout a 24 h period). We focused on the metabolic pathways involved in TG synthesis, that have been investigated at the functional level and at different periods of a day, according to the circadian rhythmic expression of related metabolic proteins and transcripts. We also analyzed the impact of an absence of RORα on its core clock partners expression pattern. Finally, we tested, in WT mice, the in vivo effect of a RORα inverse-agonist (SR3335) on hepatic TG synthesis, and on gluconeogenesis, in order to mimic the metabolic daytime-dependent phenotype of the sg/sg mouse with a pharmacological approach.

Results and discussion

Metabolic blood parameters and hepatic TG content are improved throughout the day in the RORα-KO (sg/sg) mice

We examined the role of RORα in lipid and glucose homeostasis throughout the day by collecting samples every 4 h over a period of 24 h -mice exposed to light for 12 h, from ZT0 to ZT12, and in darkness for 12 h, from ZT12 to ZT24 (Fig. 1). The circadian fluctuations of these parameters in WT mice corroborated those previously described[24]. In sg/sg mice, only experiments performed in the light period have been published and reported lower levels of hepatic TG content, plasma TG and glucose concentrations when compared to WT mice[8,9,12]. Our data confirmed such pattern during the light period and illustrated, for the first time, that the same profile persisted during the night period. Overall, the circadian variation in lipid homeostasis seemed to be preserved in the sg/sg mice, but with lower amplitude than in WT mice. Since L-RORαγ-KO revealed time-dependent impact of RORs on lipogenic gene expression and TG content[23], we focused our analysis on pathways involved in hepatic TG synthesis over a full circadian cycle.

Triglyceride synthesis was altered in the liver of sg/sg mice, in a time-dependent way

Hepatic TG synthesis includes free fatty acid (FFA) esterification into TG, and FFA synthesis from hexoses (de novo lipogenesis). The first process requires the synthesis of glycerol-3-phosphate (G3P) from various substrates according their availability: pyruvate and glycerol during the fasting period, and glucose when insulinemia increases compared to cAMP. Lipogenesis includes glycolysis as a first step, and de novo lipogenesis producing FFA from acetyl-CoA. The lipogenic pathway was studied at a functional level (Fig. 2a), and compared with the expression of related proteins (Fig. 2b) and transcripts (Fig. 2c).

Glyceroneogenesis (GNG) is a truncated pathway of gluconeogenesis which provides G3P from lactate and pyruvate, and phosphoenolpyruvate carboxykinase (PEPCKc) is its rate-limiting enzyme. We previously showed that GNG was functionally reduced in adipocytes of sg/sg mice, due to the combined decrease of the *PCK1* gene expression, PEPCKc protein levels and its specific activity[15]. Given that GNG also significantly takes place in the liver[25], we functionally assessed hepatic GNG by measuring the incorporation of $^{14}C_1$ pyruvate into TG in freshly prepared liver samples. GNG was decreased in the sg/sg compared to WT mice at ZT10, *i.e.* in the light and fasting period, but not at ZT0, *i.e.*at the end of the night and fed period (Fig. 2a, left panel). Quantification of the relative amount of PEPCKc confirmed a rather constant decrease in the protein expression all along the 24 h period, with a conserved circadian rhythm (Fig. 2b, left panel); the *PCK1* transcript cycled accordingly, with lower amplitude mostly in the light period (Fig. 2c, left panel). This data confirms that RORα is a physiological trans-activator of *PCK1*[19], required for maximal gene expression, but not for its cycling in the liver.

Glycerol, derived from TG lipolysis in adipocytes, is another substrate used for synthesis after its phosphorylation by glycerol kinase (GyK). Analysis of U-^{14}C glycerol incorporation into TG showed a significant increase at ZT0, that was no more significant at ZT10, in the liver of sg/sg compared to WT mice (Fig. 2a, left panel). Accordingly, the amount of GyK proteins level was slightly enhanced in the liver of the sg/sg mice in the light period (Fig. 2b, left panel). By contrast, the *GyK* transcript abundance appeared equal or lower in sg/sg compared to WT mice (Fig. 2c, left panel), suggesting some stabilization of the protein in the liver of the sg/

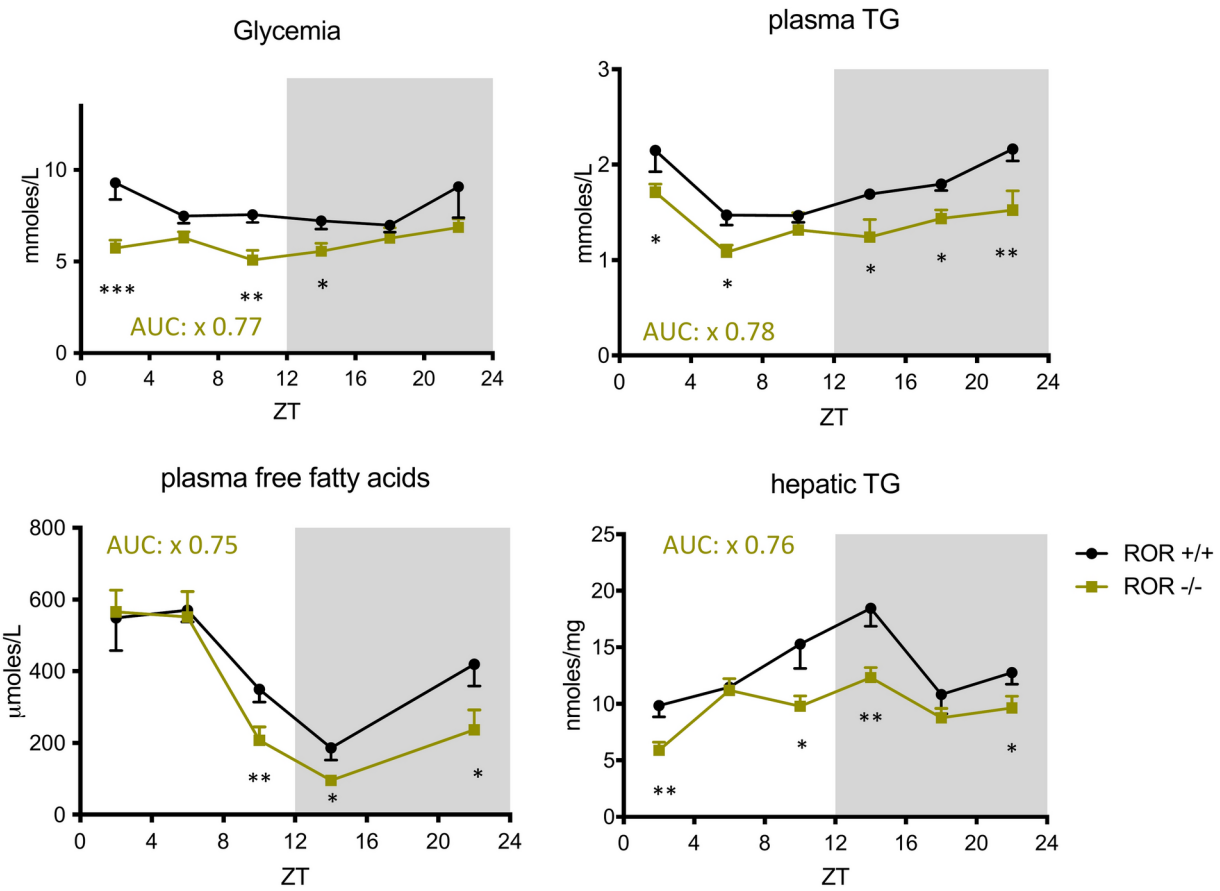

Fig. 1. Metabolic blood parameters and hepatic TG content are improved throughout the day in the RORα-KO (sg/sg) mice. RORα + / + and −/− mice, weighing 29.6 + /− 0.9 and 23.9 + /− 1.5 g respectively, were compared. Plasma and liver samples have been isolated from mice fed a standard chow diet ad libitum and killed at 4 h intervals over 24 h at 12:12 h light/dark condition (n = 6 mice per point) and tested for plasma glucose, TG, FFA and hepatic TG. The area under the curve (AUC) in sg/sg (green) *vs* WT (black) mice is mentioned when different by at least + /− 20%. ZT refers to "Zeitgeber Time", ZT0 and ZT12 defining the time of lights on and down (materialized by gray shading), respectively. Data presented as mean + /−SD; two-way ANOVA with Bonferroni post-hoc test: $^{*}P < 0.05$, $^{**}P < 0.01$, $^{***}P < 0.001$ sg/sg *vs* WT.

sg mice. Finally, glycerol was used about 3-times less than pyruvate for supplying G3P at ZT10 (Fig. 2a); this confirms GNG as the major pathway for G3P synthesis in the rest period of mice[25].

Glucose is a shared substrate for both G3P and FFA synthesis through glycolysis. We compared the incorporation of U-^{14}C glucose into TG in the liver of both sg/sg and WT genotypes at three time points over a 24 h period (Fig. 2a, mid panel). We detected a sharp reduction of glucose incorporation into TG at ZT4 in the liver of sg/sg compared to WT mice, still noticeable at ZT12 although not significant. Western blot analysis of the glycolysis limiting enzyme, L-Pyruvate kinase (L-PK), confirmed a marked decrease of the protein amount in sg/sg *vs* WT mice, in particular during the light period (Fig. 2b, mid panel). The circadian rhythm of the *PKLR* transcript seemed to be preserved in the absence of RORα with a peak at ZT14, similar to that of WT mice[26], although with a dampened amplitude (Fig. 2c, mid panel).

Finally, to by-pass the glycolytic step and investigate the impact of RORα on de novo lipogenenesis only, we tested the incorporation of U-^{14}C acetate as a precursor of FFA synthesis in the light and the dark periods. In sg/sg mice, we observed a sharp decrease of acetate incorporation into TG at ZT6 and no difference between the genotypes at ZT18 (Fig. 2a, right panel). In WT mice, de novo lipogenesis was found to be higher at ZT6 than at ZT18; this corroborates data showing that the peak of TG accumulation in the liver occurs around ZT8[27]. Western blot analysis of two major actors of lipogenesis—Acetyl-coenzyme A-carboxylase (ACC) and fatty acid-synthase (FAS)—revealed mild rhythmic variation of these proteins throughout the day, with the highest amount occurring at ZT22 in WT mice (Fig. 2b, right panel). The pattern in sg/sg mice was rather similar to that of the WT counterparts except at ZT6, where ACC and FAS levels were reduced. This lower level of ACC and FAS protein content in sg/sg mice did correspond to the nadir of their transcript at ZT6 (Fig. 2c, right panel and[8].

Our functional approach demonstrated for the first time that the whole body RORα-KO leads to an altered hepatic TG synthesis that is restricted to the light period and impacts several pathways: glycolysis and de novo lipogenesis for the synthesis of FFA, and GNG for their subsequent esterification into TG. Such data corroborated some reported decrease of *PCK1*, *PKLR* and *FAS* transcripts in the liver of sg/sg mice[15], presumably performed

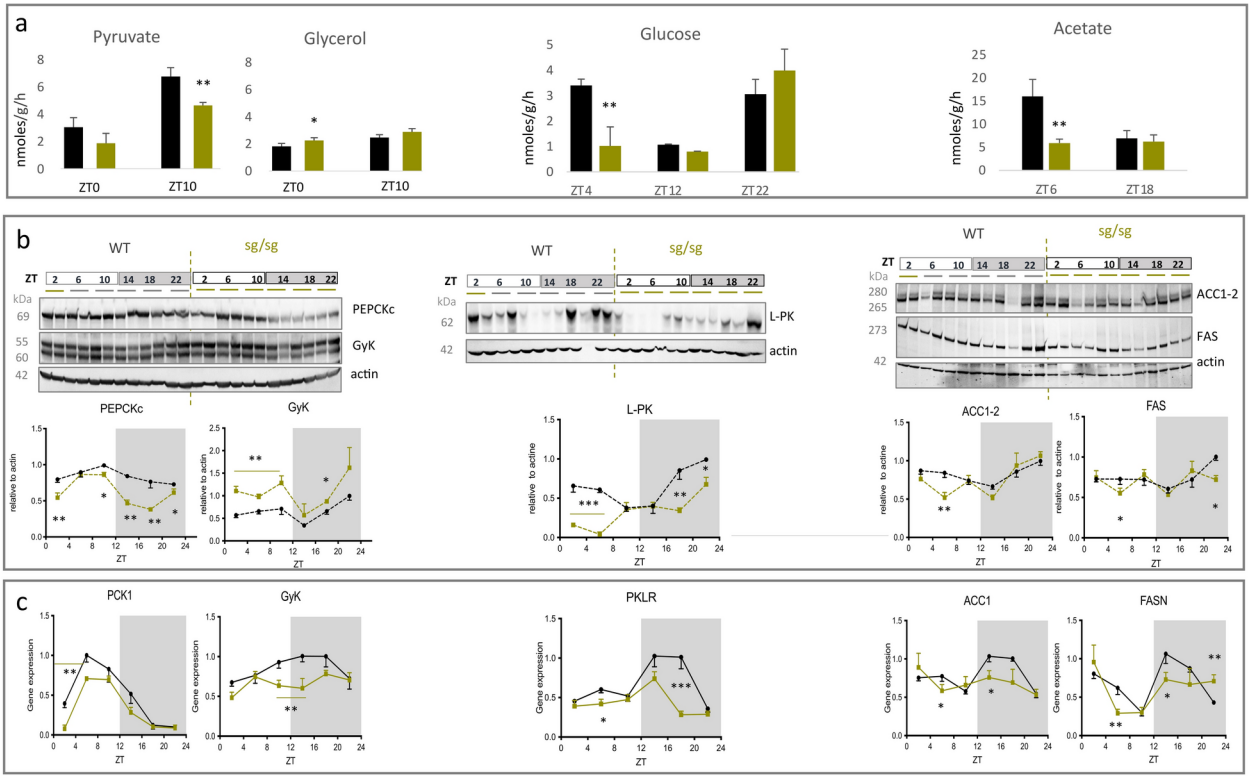

Fig. 2. Triglyceride synthesis was altered in the liver of sg/sg mice, in a time-dependent way. (**a**) Functional analysis of radiolabeled substrates (pyruvate, glycerol, glucose or acetate) incorporation into TG in liver explants of sg/sg (green) and WT (black) mice at different periods of the day. The experimental time points were chosen according to the expression profile of the proteins involved in the relevant pathways. Concerning night points (ZT18, ZT22 and ZTO), mice were previously housed in inverted light cabinets for two weeks prior to the experiment. The tests were performed in duplicate on livers from 4 mice and means were compared by unpaired Student 's t test. $*P<0.05$, $**P<0.01$, sg/sg *vs* WT. (**b**) Representative western blots and protein content normalized to actin in liver samples from sg/sg and WT mice, over a 24 h period. Tissues from two mice were pooled at each time point. The relative abundance of each protein was expressed as a percentage of the peak value in WT mice (n = 4). WT in dotted black line and sg/sg in green. (**c**) Daily pattern of corresponding transcripts (n = 6 mice per point). The relative abundance of each mRNA was normalized to three housekeeping genes and expressed as a percentage of the WT acrophase. WT in black and sg/sg in green. Data presented as mean + /-SD; two-way ANOVA with Bonferroni post-hoc test: $*P<0.05$, $**P<0.01$, $***P<0.001$ sg/sg *vs* WT.

at light[8,11]. Given that RORα and/or RORγ are recruited to ROREs in several key genes involved in glucose homeostasis and lipid metabolism, including *PCK1, PKLR* and *FAS*[11], one possibility to explain their decreased transcription in the liver of sg/sg mice in the light period is as a direct consequence of the local loss of RORα transcriptional activity. RORα would then be an effector of the cycling of these pathways. However, *FAS* and *ACC* transcripts did not vary in two studies of L-RORα-KO mice fed a chow diet[21,22]—with one showing a trend to decrease, and no mention made of the timing of the analysis in the other[22]. This does not point to a liver-autonomous mechanism.

Given RORα belongs to the core clock machinery, his absence had potential consequences on the circadian rhythm and/or expression of its clock partners. This was important to delineate as clock genes can themselves control some metabolic genes[24].

RORα is necessary for robust circadian rhythm of core clock gene expression and its loss of function led to rhythmic disruption in Reverbα protein amount

Amongst the core clock genes family, *Bmal1*, *Clock* and *Cry1* are direct target genes of RORs, but not *Per2*[28]. Accordingly, our data depicted their dampened transcript level in sg/sg mice, with no alteration in their rhythmicity (excepted a 4 h-delayed peak of *Bmal1* transcript) while *Per2* expression was not affected (Fig. 3a). Consequently, Bmal1 and Clock protein amounts were decreased at ZT6 (Fig. 3b), as expected for true targets of RORα. We also assessed the ROR family, both at the transcript (Fig. 3a, right panel) and the protein (Fig. 3b) levels over a 24 h period. The complete lack of the RORα protein in sg/sg mice was confirmed by western blot (Fig. 3b). Our data further revealed that, in WT mice, RORα protein content exhibited a marked rhythmic expression with a peak at ZT22 (Fig. 3b), though it remained arrhythmic at the transcript level (Fig. 3a) and[5]. The *RORγ* transcript showed a robust oscillatory pattern with a peak during the night in the two genotypes,

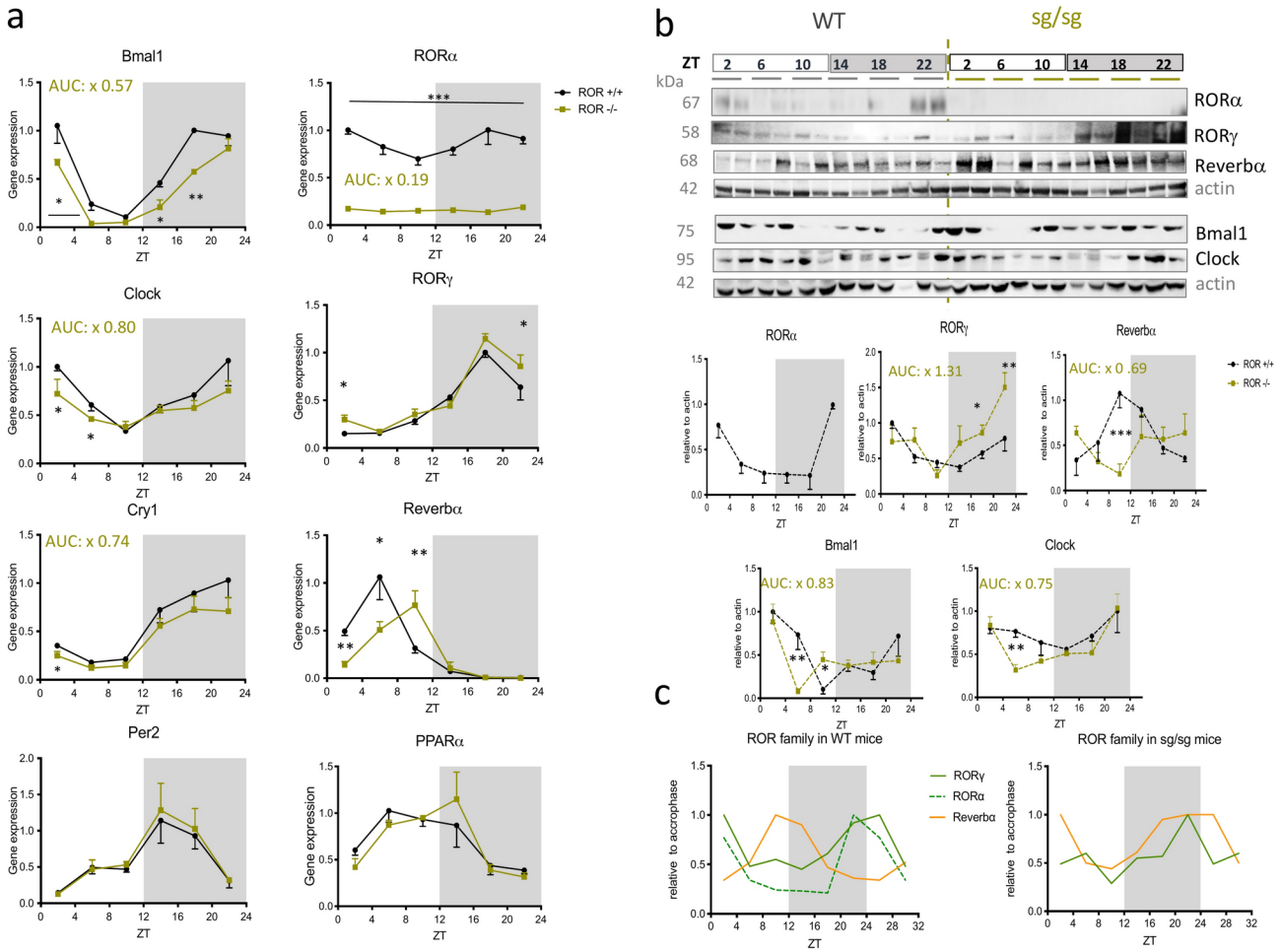

Fig. 3. RORα is necessary for robust circadian rhythm of core clock gene expression and its loss of function led to rhythmic disturbances in Reverbα protein amount. Mice fed a standard chow diet ad libitum were killed at 4 h intervals over 24 h at 12:12 h light/dark condition (n = 6 mice per point). AUC was reported when found to be statistically different between the two genotypes. (**a**) Core clock gene and ROR family transcripts were normalized to three housekeeping genes and their relative expression was referred to the acrophase of WT mice. WT in black and sg/sg in green. (**b**) Representative western blots of total liver lysates from mice sacrificed every 4 h (tissues from two mice were pooled at each time point) and below, the protein intensity normalized to actin as the loading control of each point and represented as % of WT peak (n = 4). WT in dotted black line and sg/sg in green. (**c**) Representation of the ROR family members rhythmic profiles in each genotype. Values are from section (b). Data presented as mean + /−SD; two-way ANOVA with Bonferroni post-hoc test: $^{*}P < 0.05$, $^{**}P < 0.01$, $^{***}P < 0.001$ sg/sg *vs* WT.

with a weakly extended peak (significant increase at ZT22 to ZT2) in sg/sg compared to WT mice (Fig. 3a), as previously suggested in various RORα-KO models[9,21,23]. Accordingly, the RORγ protein amount was increased (by 1.3-fold) in sg/sg mice with higher levels at night (Fig. 3b). The *Reverbα* transcript and protein exhibited marked cyclic expression in WT mice, peaking at ZT6 (Fig. 3a) and ZT10 (Fig. 3b), respectively[6]. By contrast, the RORα deletion led to a 4 h-shift of the transcription of *Reverbα* (Fig. 3a), followed by a 4 h-delay and dampening of its protein expression profile during the night (Fig. 3b). A mild decrease of *Reverbα* transcript level at ZT4 in sg/sg mice[29] and in L-RORα-KO[21] were already noted, but its circadian protein pattern in the liver of RORα-KO mice was never published, although Reverbα is a well-known RORα-target[30].

Finally, the circadian pattern of the ROR family members was compared within each genotype (Fig. 3c). In WT mice, RORα and RORγ protein peaked in phase and were anti-phasic with their trans-dominant negative partner, Reverbα. These protein profiles perfectly fit their DNA binding activity—between ZT22 and ZT6 for RORs and at ZT10 for Reverbα[31]. That depicts how some RORE-target genes are cycled over the 24 h period: activated by RORs in the light period then repressed by Reverbα in the night. By contrast, in sg/sg mice, the Reverbα protein profile was abnormally in phase with RORγ (Fig. 3c, right panel), thus potentially competing for shared RORE-binding sites on target genes[32] and neutralizing their action in the night. Such a scenario could contribute to the failure of RORγ to replace RORα in sg/sg mice, at least with regards to common target genes.

In summary, our data confirm a cyclic profile of the RORα protein, as previously documented[33], reinforcing the notion that RORα is a meaningful actor in the hepatic circadian control of gene expression. Indeed, its

deletion in sg/sg mice lead to a 4 h-delay in peaks of *Bmal1* and *Reverbα* transcripts and a modest RORγ over-expression. This suggests that RORα is more efficient than RORγ in promoting the transcription of these two target genes[29,30]. The modified protein pattern of Bmal1 could alter those of *PKLR* and *Reverbα*, which are direct targets of Bmal1[6,26]. Subsequently, the loss in the counter-regulation exerted by Reverbα in a suitable timeframe could up-regulate *RORγ*[34] and possibly have also some effect on lipogenesis, since Reverbα controls the diurnal rhythm of de novo lipogenesis in hepatocytes[35].

Disturbances in rhythmic expression of transcription factors involved in lipogenesis in sg/sg mice.

Given the increased lipogenesis observed at night in L-RORαγ-KO mice[23], we focused on the molecular pathways that regulate lipogenesis according the time of the day in sg/sg mice. We first checked the circadian expression profile of three major transcription factors governing lipogenesis (Fig. 4a). Liver-X receptor (LXRα) and carbohydrate response element-binding protein (Chrebpα) are both critical regulators of sterol regulatory element-binding transcription factor (Srebp1c), that further mediates the insulin response to lipogenic gene transcription.

In accordance with the decreased lipogenic capacity observed in sg/sg mice during the light period (Fig. 2a), *Srebp1c* and *LXRα* gene expression decreased at this period in sg/sg mice (Fig. 4a). Given RORα binds the *Srebp1c* promoter[8], the reduced expression of *Srebp1c* transcript at this period could be a direct consequence to the lack of RORα in sg/sg mice. Accordingly, a direct Srebp1c target gene, *SCD1,* was decreased in one L-RORα-KO model[22], suggesting a cell-autonomous process of regulation.

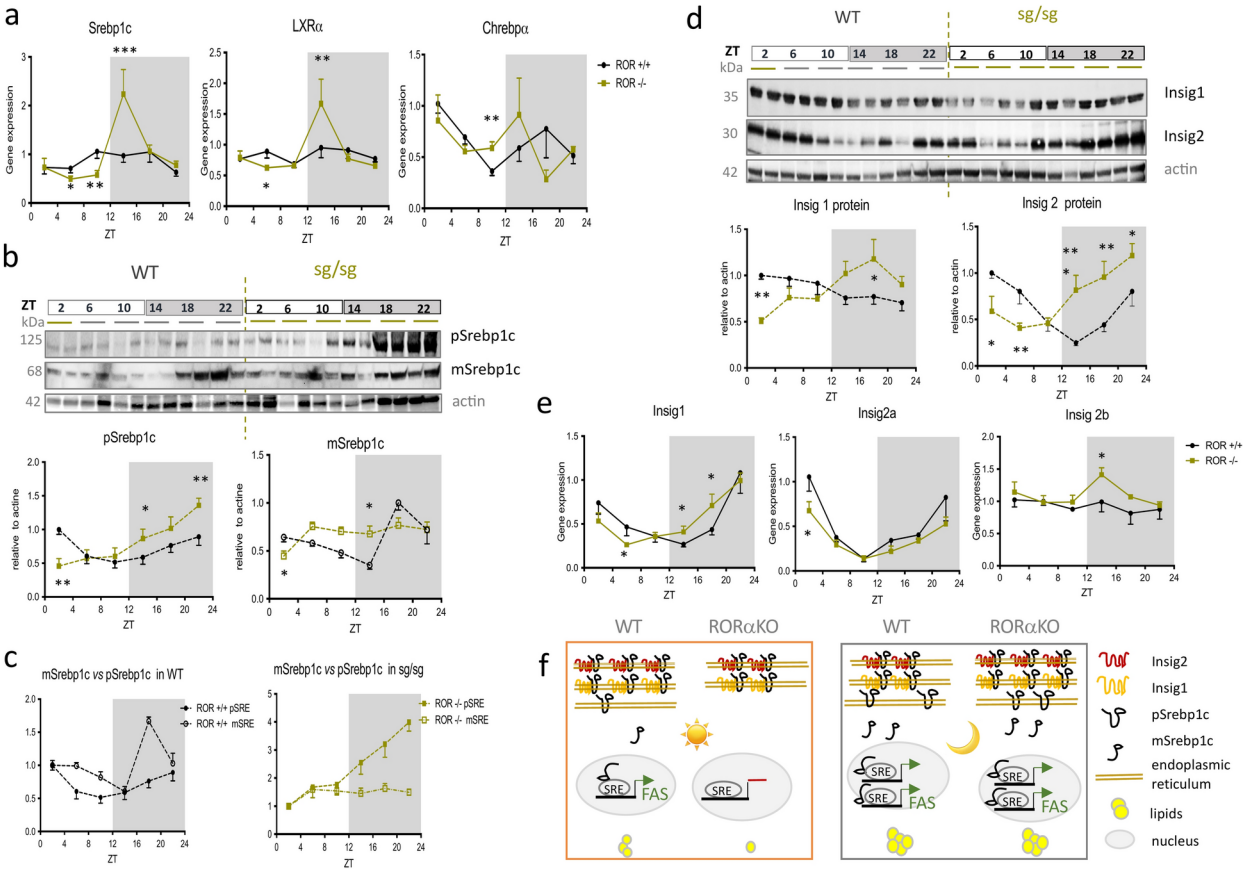

Fig. 4. Disturbances in rhythmic expression of transcription factors involved in lipogenesis in RORα-KO (sg/sg) mice. **(a)** and (**e**) Daily pattern of transcripts in liver samples from sg/sg or WT mice, over a 24 h period. WT in black and sg/sg in green (n = 6). (**b**) and (**d**) Representative western blots and protein contents normalized to actin in liver samples from sg/sg (dotted green line) and WT (dotted black line) mice, over a 24 h period. Tissues from two mice were pooled at each time point. Data presented as mean + /−SD; two-way ANOVA with Bonferroni post-hoc test: $^{*}P < 0.05$, $^{**}P < 0.01$ sg/sg *vs* WT. (**c**) Illustration of the relative amounts of pSrebp1c (full mark) and mSrebp1c (open mark) in each genotype (WT in black) or (sg/sg in green). (**f**) Proposed schema of the homeostasis between pSrebp1c expression and mSrebp1c activation in RORα-KO (sg/sg) *vs* WT mice in the light and the dark period. At light (left panel), simultaneous decrease of pSrebp1c, Insig1 and Insig2 proteins in RORα-KO mice; if they are in stoichiometric proportions, thus sequester pSrebp1c in endoplasmic reticulum with no lipogenesis. At night (right panel) in RORα-KO mice, the increase of pSrebp1c overcomes that of Insig1 and Insig2 proteins, allowing similar mSrebp1c maturation and lipogenesis than in WT mice.

By contrast, at night, despite similar lipogenic capacities between the two genotypes (Fig. 2a), an early peak of *Chrebp*α mRNA was noted in sg/sg mice, possibly linked to their relatively early daily food intake[13], as well as some transient over-expression of *Srebp1c* and *LXR*α transcripts at ZT14 (Fig. 4a). Physiologically, *LXR*α gene expression is not cycling[27] but activated by metabolic ligands[36]. The *LXR*α increased transcription in sg/sg mice is explicable since RORα is able to interrupt the autoregulatory loop of LXRα[37]. The fact that this increase was never seen before is probably due to the timing of previous analyses[8,38]. The increase of *Srebp1c* transcript at ZT14 in sg/sg mice could therefore result from LXRα increase, since the promoter for *Srebp1c* contains LXR-binding sites[39]. *Srebp1c* transcription is also driven by clock genes[40]. In particular, Reverbα binds *Srebp1c* promoter under physiological conditions[41]. Thus, the unusual lack of Reverbα at the end of the light period in sg/sg mice (Fig. 3b) could result in a loss of *Srebp1c* inhibition at that time.

In summary, our data confirms that RORα and Reverbα take part in the rhythmic control of *Srebp1c* gene expression, as activator (during the day) and inhibitor (at night), respectively, according their alternative circadian expression. Moreover, RORα seems necessary to interrupt the autoregulatory loop of LXRα, and its unusual transactivation at night in sg/sg mice could further increase *Srebp1c* transcription.

To investigate the discrepancy between the levels of *Srebp1c* transcript and those of its target genes at night in sg/sg mice, we assessed the levels of both its precursor (pSrebp1c) and its nuclear-cleaved form (mSrebp1c) by western blot over the 24 h period. Indeed, Srebp1c is synthesized as an inactive precursor and remains in the endoplasmic reticulum by the intervention of "Insulin-induced genes" (Insigs) that exert a negative feedback control on lipogenesis. The complex of pSrebp1c-Insig prevents the migration of pSrebp1c to the Golgi apparatus, where the necessary proteases for its proteolytic activation into mSrebp1c are located. mSrebp1c is then able to translocate to the nucleus (Fig. 4f). According to the pattern of *Srebp1c* transcript (Fig. 4a), pSrebp1c accumulated more in the liver of sg/sg than in WT mice during the night period (Fig. 4b). However, although mSrebp1*c* expectedly rose at ZT18 in WT mice, its amount stayed rather stable in sg/sg mice from ZT6 to ZT22, excepted at ZT2 where it was decreased compared to WT mice. The illustration of their respective amounts in each genotype (Fig. 4c) hinted at an alteration of the processing of pSrebp1c into its mature form in sg/sg mice during the night.

There are two Insig isoforms that are rhythmically expressed in the liver, but they are distinctive by their regulation and half-lives[42]. In sg/sg mice, the peaks of Insig1 and Insig2 proteins were early (by 8 h and 4 h, respectively) compared to WT mice (Fig. 4d). Therefore, the increased amount of both Insigs at night in sg/sg mice possibly contributes to prevent the maturation of pSREBP1c into mSREBP1c at that time, as a counter-regulatory process on de novo lipogenesis. Their altered expression in sg/sg mice would be, at least partly, due to transcriptional events. Indeed, sg/sg mice exhibited both an early increase of *Insig1* transcript, as well as a relative increase of *Insig2b* transcript at ZT14 (Fig. 4e).

Insig1 is closely associated with lipogenic genes[43]; its transcription requires mSREBP1c[44] and, accordingly, was delayed by about 8 h, compared to that of mSREBP1c in both genotypes. Insig2 could be translated from two transcripts, Insig2a being liver-specific and Insig2b ubiquitous[42]. Our data showed that the increase of the Insig2 protein at night in sg/sg mice results from the increase of *Insig2b* transcript (Fig. 4e). The observation of some over-expression of *Insig2b* in L-RORαγ-KO mice[23] suggests a liver-autonomous mechanism due the lack of RORα. Insig2a is a specific RORγ target[38] and inhibited by Reverbα[45]. Unexpectedly, *Insig2a* transcript was decreased at ZT2 in sg/sg compared to WT mice (Fig. 4e). This could reflect the competition between RORγ and Reverbα that were found to be abnormally co-expressed at ZT22 in sg/sg mice (Fig. 3c), leading to the decrease of *Insig2a* transcript at ZT2 (Fig. 4e), and then of its protein at ZT2 to 6 (Fig. 4d).

In summary, disruptions in the rhythmic expression of transcription factors involved in hepatic lipogenesis were noted in the whole-body RORα-KO mice. *LXR*α and *Srebp1c* transcription profiles were more cyclic in sg/sg than in WT mice (decreased in the light period, and increased at the beginning of the night period). However, the subsequent pSREBP1c over-expression at night did not drive any increased lipogenesis in sg/sg mice because Insig1 and 2 proteins increased simultaneously, prohibiting its processing into mSREBP1c (see Fig. 4f for a schematic representation). The increase of both *Srebp1c* and *Insig2b* gene transcription was also observed in L-RORαγ-KO mice[23], suggesting a liver autonomous mechanism of regulation by RORα.

Pharmacological antagonism of RORα in WT mice mimics the time-dependent metabolic variations observed in the liver of sg/sg mice

Given the whole-body RORα-deletion decreased hepatic TG synthesis in the day period, we decided to pharmacologically modulate RORα in WT mice, expecting to mimic the benefits observed in the lipid metabolism of sg/sg mice during the day period. We already used the selective RORα inverse agonist SR3335 to increase adaptive thermogenesis and decrease fat mass in C57Bl/6 J mice in vivo[17]. We started by assessing relevant parameters in these C57Bl/6 J mice treated with four consecutive intra-peritoneal doses of SR3335. The RORα inverse agonist decreased their TG content in the liver (Fig. 5a) and plasma (Fig. 5b), and increased plasma glycerol concentration (Fig. 5b), suggesting an activation of adipose lipolysis.

To explain the causes of the loss of liver TG content in response to SR3335, hepatic lipogenesis was functionally tested through the analysis of U-^{14}C glucose incorporation into TG in freshly prepared liver slices from SR3335- or DMSO-treated sg/sg and WT mice around ZT4-6. Figure 5c shows that one single SR3335 injection at ZT0 (around the daily peak of RORα protein amount, see Fig. 3b) was sufficient to cause a decrease, 28–30 h later, in the hepatic lipogenesis of WT mice. This took place to a level comparable to that observed in sg/sg mice. This downregulation did not occur in the SR3335-treated sg/sg mice and thus was RORα-specific. The liver samples from these mice were analyzed by western blot to further delineate the proteins influenced by SR3335. As anticipated, SR3335 led to a reduction in the level of mSREBP1c by half in WT and not in sg/sg mice around ZT4-6 (Fig. 5d) A similar reduction in FAS and L-PK in WT mice in response to SR3335 was observed, with no significant change in sg/sg mice. We also assessed the impact of SR3335 on hepatic TG content and

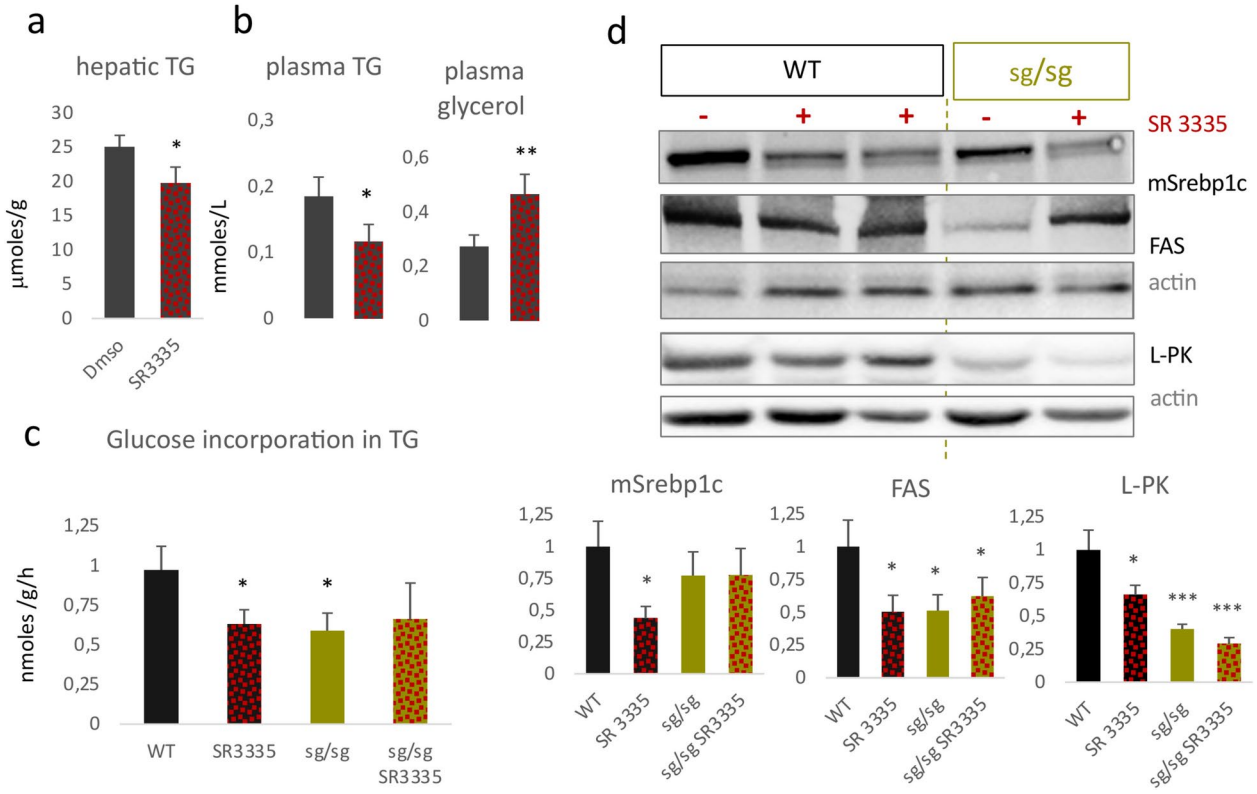

Fig. 5. Pharmacological antagonism of RORα in WT mice mimics the time-dependent lipogenic variations observed in RORα-KO (sg/sg) mice. **(a)** Hepatic TG content and **(b)** Plasma TG and glycerol content in C57Bl6/J mice (19-wk-old female weighing 23.9 + /− 1.1 g) treated with DMSO (control in black) or the RORα inverse agonist (SR3335 in red on black), 10 mg/kg/day for 4 consecutive days. Samples (n = 6) were collected at ZT9-12. **(c)** Functional analysis of de novo lipogenesis by the measure of U-^{14}C glucose incorporation into TG in liver explants from male WT mice treated with DMSO (control in black) or RORα inverse agonist (SR3335 in red on black) and, from sg/sg mice treated with DMSO (control in green) or RORα inverse agonist (SR3335 in red on green). SR3335 (10 mg/kg) was intra-peritoneally injected once at ZT0, the liver samples were analyzed at ZT4-6, the day after (n = 4–8 per condition). **(d)** Representative western blots and protein contents normalized to actin in liver samples from sg/sg and WT mice from (c)section, treated with DMSO (control) or SR3335 and collected at ZT4, (n = 4). Means + /-SD were compared by unpaired Student 's t test. $^{*}P < 0.05$, $^{**}P < 0.01$, $^{***}P < 0.001$ sg/sg *vs* WT.

lipogenic actors at ZT22 (Supplementary Fig. 1). As expected, SR3335 did not alter the lipogenic protein amount (mSrebp1c, FAS and L-PK), nor the liver TG content in WT mice during the night.

Gluconeogenesis was previously shown to be decreased in male sg/sg compared to WT mice, with a lower rise in glycemia in response to a pyruvate injection (pyruvate tolerance test, PTT)[15]. Here, we obtained similar results with female sg/sg mice, in which glycemia was comparatively lower than in WT mice from T0 (overnight fast) until one hour after the pyruvate injection (Fig. 6a). We further examined the effect of SR3335 in vivo on PTT results. Figure 6a shows that one single SR3335 injection was able to decrease both the glycemia of WT mice after an overnight fast (T0), and their capacity to de novo synthesize glucose from pyruvate for at least 30 min. As expected, SR3335 injection had no effect on PTT results in sg/sg mice. Furthermore, we investigated the capacity of SR3335-treated mice to produce glucose from liver explants ex vivo. The hepatic glucose production was significantly decreased in WT mice in response to SR3335, but not in sg/sg mice (Fig. 6b). At the same time, the PEPCKc protein amount was decreased in the liver of SR3335-treated WT mice, while SR3335 had no effect on this protein in sg/sg animals (Fig. 6c).

Given antagonizing RORα lead to a decrease in both gluconeogenesis and lipogenesis in the day period, we posited that activating RORα should exert an opposite effect. We tested a ROR-agonist, SR1078, on these pathways (Supplementary Fig. 2). A single SR1078 injection increased glucose neo-production (by 1.3-fold) and glucose incorporation into TG (by 1.5-fold) in liver explants from WT mice at ZT10, without any effect on sg/sg mice. Alongside this, their liver samples exhibited a two-fold increase of FAS and L-PK protein expression in WT but not in sg/sg mice.

Taken together, this data illustrates how the RORα-inverse agonist SR3335 can mimic in vivo the impact of the full RORα deletion both on lipid and glucose hepatic metabolic pathways. This translates to reduced rates of lipogenesis and gluconeogenesis in the day period of SR3335-treated WT mice, without any variation at

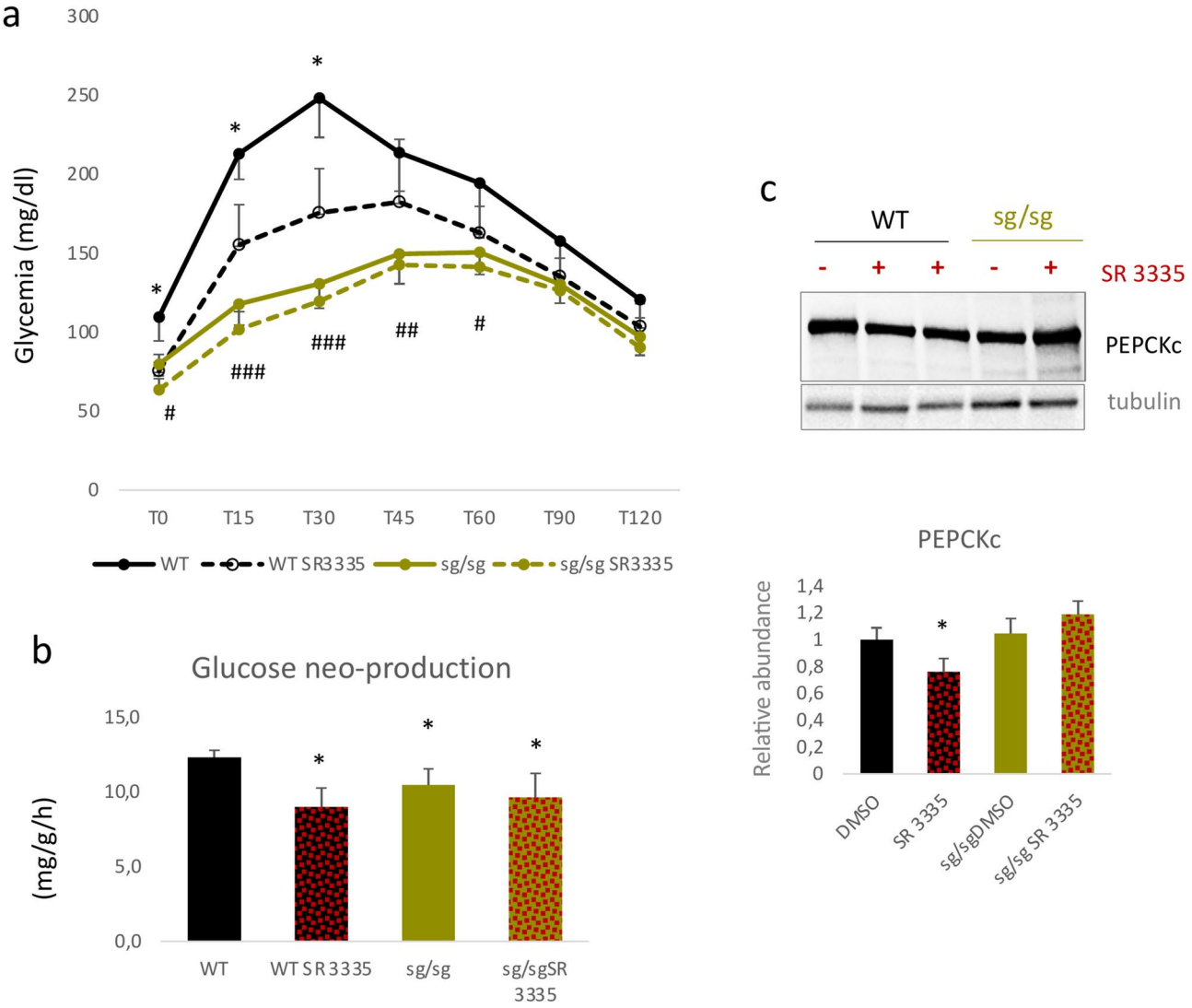

Fig. 6. In vivo effect of a RORα inverse agonist on glucose homeostasis. **(a)** Functional pyruvate tolerance test (PTT), assessing plasmatic glucose levels in response to pyruvate injection (2 mg/kg) in female sg/sg and WT mice, treated with DMSO (control) or the RORα inverse agonist (SR3335, 15 mg/kg) 16 h before the test that was performed between ZT2-4 (n = 6). Mice were aged (between 12 to 18 months-old), the WT weighing 25.3 + /− 0.9 g and sg/sg 20.4 + /− 1.6 g. Means + /−SD were compared by unpaired Student 's t test. *$P < 0.05$ SR3335-treated WT *vs* DMSO-treated WT, #$P < 0.05$, ##$P < 0.01$, ###$P < 0.001$ sg/sg *vs* WT. **(b)** Functional assay of glucose secretion by liver explants from sg/sg and WT mice, pre-treated with DMSO (control) or RORα inverse agonist (SR3335). Two doses (10 mg/kg/day), 24 and 48 h before the test that was performed at ZT9-10. (n = 4–6). **(c)** Representative western blot of PEPCKc in liver samples from sg/sg and WT mice, treated with DMSO (control) or RORα inverse agonist (SR3335) from b) section. Below, quantification of PEPCKc protein content normalized to actin (n = 4–6). Means + /− SD were compared by unpaired Student 's t test. *$P < 0.05$ sg/sg *vs* WT.

night. The noted opposite effect obtained with a ROR-agonist further confirms how RORα acts as an important physiological cyclic modulator of liver function.

Conclusion

Our functional approach demonstrated how the whole-body RORα-KO decreases liver TG synthesis (through decreased glyceroneogenesis, glycolysis and de novo lipogenesis) only during the light period, and without an increase in the dark period of mice fed ad libitum. Moreover, the observation that this time-dependent scenario was pharmacologically reproducible by the RORα-inverse agonist SR3335 in WT mice and not in sg/sg mice, supported a RORα-related mechanism. Together with the opposite observations made with a ROR-agonist, this points towards RORα contributing in a cell-autonomous manner to the circadian control of *Srebp1c, FAS, ACC, PK-L* and *PEPCKc* gene transcription, especially as these genes were identified as bound to, or controlled by RORs[8,11]. However, the transcription level of some of these genes, having been analyzed in L-RORα-KO models (*Srebp1c,*

FAS, ACC), was not changed or only mildly diminished in the light period[21,22]. One could point to inappropriate timing of assessments, but these L-RORα-KO mice do not exhibit lower TG content[21,22], or improved PTT[21]. They do not possess the same liver phenotype as whole-body RORα-KO (sg/sg) mice. Our impression is that these metabolic genes are true molecular targets of the couple RORα/Reverbα in the liver, but their cyclic control by clock genes could be meaningful only in specific situations, such as a low FFA availability and/or a misfeeding (increased daily food intake) which are only observed in the whole-body RORα-KO mice. Indeed, sg/sg mice exhibit increased FFA oxidation in fat and muscle[12,16,20], thereby modifying the strong temporal correlation of FFA across tissues[46]. Furthermore, the inhibitory control of Reverbα against certain fluctuations of lipogenesis[35,45] only became evident in one study, in a context of mistimed feeding during the day time (food intake from ZT4 to 8)[47]. Collectively, this suggests that RORα fines-tune lipogenesis, with an up-regulation in the day, and a down-regulation at night.

Mechanistically, we demonstrated a strong circadian cycling of the RORα protein in the liver. Its deletion induced a phase-shifted expression of its targets *Bmal1* and *Reverb*α, as suggested in RORαγ-KO mice models – both in whole body[29] and liver-specific[21,23] fashion. The phase-shifting of Reverbα in particular, would further deregulate the *Srebp1c/Insigs* pathway, as observed in Reverbα-KO mice[45]. However, in sg/sg mice, the increased *Srebp1c* transcription at night was counteracted because of the early overexpression of both Insigs (see Supplementary Fig. 3). Finally, our data confirmed a role of RORα in the inhibition of *LXRα* transcription[37], which could further control *Srebp1c* expression and lipogenesis at night. We hypothesized that the increased TG liver content observed at night in L-RORαγ-KO was related to the combined consequence of the lack of RORα (which caused increased *Srebp1c* transcription) and the lack of RORγ (which decreased *Insig2a* transcription), thereby leading to its maturation into mSrebp1c (see Supplementary Fig. 3). The LXRα increase at night in RORα-KO mice possibly explains why the L-RORα-KO mice develop steatosis after high fat diet[22]. This is not the case in global RORα-KO[8], because of simultaneous increased FFA oxidation in others organs[12,16,20]. Taken together, this illustrates how it might be more metabolically beneficial to reduce RORα expression throughout the whole body rather than just in the liver. This supports the rational use of a pharmacological RORα-blockade to prevent pathologies affecting metabolic pathways. This can be achieved by natural RORs inverse-agonists, such as vitamin D hydroxyderivatives[48,49]. However, this mediation could be restricted to subjects benefiting from a rather healthy diet and without proven steatosis. Indeed, in a model of obesity or western-diet feeding background, it seemed most relevant to focus on RORα activation (and not inhibition). Firstly, liver-specific RORα-deficient mice develop hepatic steatosis only when challenged by a high fat diet[22]. Secondly, nobiletin, a natural flavonoid acting as a ROR-agonist, improves liver steatosis in obese mice but without any effect on mice fed a standard chow diet[50]. In such pathologic circumstances, some of the benefits mediated by an activation of RORα-mediated pathways could result from its anti-inflammatory properties[51]. We, themselves, have previously described an anti-inflammatory role for RORα in response to a Western Diet feeding, but not in chow diet-fed mice[14].

Methods

Animals and tissue collection

The staggerer (RORα sg/sg) mutant mouse was maintained on a C57BL/6 J genetic background. Heterozygous sg/ + have been kindly provided by Prof. J. Mariani (Institut Gustave Roussy, Villejuif, France) and were referred to as B6.C3 (Cg-RORα ^{sg}/J) in the Jackson laboratory (Bar Harbor, ME). Generation of sg/sg mice were obtained from crossing heterozygous sg/ + mice and compared with their + / + littermates. All animals care and use procedures were conducted according to the European Communities Council Directive (2010/63/UE) and approved by the Regional Animal Care and Use Committee (Ile-de-France, Paris, no5; agreement number APAFIS#26,094–2,020,061,808,514,224 v1). We confirmed that the study was carried out in compliance with the ARRIVE guidelines, all methods being in accordance with relevant guidelines and regulations. Mice were housed in pathogen-free, temperature-controlled environment, scheduled with 12–12 h light–dark (LD) cycles (lights on from 8:00AM/ZT0) to 8:00PM/ZT12) and maintained with free access to food (A03, UAR, Epinay-sur-Orge, France) and water. Sg/sg mice were kept with their mother throughout their life and fed softened and moistened food directly placed on the bottom of the cage, as soon as one week before weaning, in order to improving their survival to similar of that of sg/ + and + / + mice. Male mice (4–6 months-old) were sacrificed by cervical dislocation at 4 h intervals over a 24 h period with four to six mice for each time point; when older and/or female mice have been used, it was specified in the figure legend. Livers were pulverized under liquid nitrogen (to exclude differences linked to the zonation of hepatocytes) and stored at − 80 °C before RNA extraction or protein lysates preparation. Blood samples were collected via cardiac puncture, under EDTA, centrifuged and plasma samples were aliquoted and snap-frozen. For in vivo treatment, mice were intra-peritoneally (IP) injected with SR3335 or SR1078 (10 mg/kg) or with the excipient [10% dimethyl sulfoxide (DMSO) and 10% Tween 80 solution].

Pyruvate tolerance test

This was performed by intra-peritoneally injecting 16 h-fasted mice with a 2 g/kg buffered pyruvate solution. Blood glucose levels were then checked every 15 min from the tail vein by using a glucometer (OneTouch, LifeScan, Issy-les-moulineaux, France).

Transcript and protein analysis

Hepatic mRNAs were extracted using the RNeasy Tissue Mini Kit (Qiagen, Courtaboeuf, France), then reverse-transcribed using the High-Capacity cDNA Reverse Transcription Kit (Applied Biosystems Carlsbad, CA, USA). Quantitative PCR of the genes of interest was performed using SYBR Green and a Light Cycler 480 Real-Time PCR System (Roche Diagnostics, Meylan, France) with specific primers listed in Table 1. Gene expression was normalized to the mean of three housekeeping mRNAs (*GAPDH*, *36B4* and *HPRT*) and data analysis was based on the DDCt method.

Gene	Primer sequences		Antibody references		
	Forward	Reverse	Proteintech	Santa-Cruz	Cell Signalling
PCK1	CAACTTCGGCAAATACCTG	CTGTCTTCCCCTTCAATCC	16754-1-AP		
GyK	GAAACTTCGTTGGCTCCTTG	CGTCCTGCTTGCATTTGTTA	13360-1-AP		
PKLR	CGAAAAGCCAGTGATGTGGTGG	GATGCCATCGCTCACTTCTAGG	22546-1-AP		
Srebf1	CCGTCACTTCCAGCTAGACC	TGAGCCTCAGCTAGGGAAAA	14088-1-AP	SC-366	
Insig1	TCACAGTGACTGAGCTTCAGCA	TCATCTTCATCACACCCAGGAC	55282-1-AP		
Insig2a	CCCTCAATGAATGTACTGAAGGATT	TGTGAAGTGAAGCAGACCAATGT	24766-1-AP		
Insig2b	CCGGGCAGAGCTCAGGAT	GAAGCAGACCAATGTTTCAATGG	24766-1-AP		
NR1f3 (RORγ)	TTTTGAGGATACCAGGCATC	CCACATCTCCCACATTGACTTC	13205-1-AP		
NR1f1 (RORα)	GCACCTGACCGAAGACGAAA	GAGCGATCCGCTGACATCA		SC-28612	
Nr1d1 (Reverbα)	AACCTCCAGTTTGTGTCAAGGT	GATGACGATGATGCAGAAGAAG		SC-393215	
ACC	AGTGCCTTCCTCGGTTTCTT	GCCAGGATTCAAGGTGTGTT			#3662
FASN	ATCCCAGCACTTCTTGATGG	CCGAAGCCAAATGAGTTGAT			#3180
Bmal1	CCACCTCAGAGCCATTGATACA	GAGCAGGTTTAGTTCCACTTTGTCT	14268-1-AP		
Clock	ACCACAGCAACAGCAACAAC	GGCTGCTGAACTGAAGGAAG	18094-1-AP		
Cry1	CTGGCGTGGAAGTCATCGT	CTGTCCGCCATTGAGTTCTATG			
Per2	TGTGCGATGATGATTCGTGA	GGTGAAGGTACGTTTGGTTTGC			
PPARα	GCACTGGAACTGGATGACAG	TTTAGAAGGCCAGGACGATCT			
LXRα	CGGGCTTCCACTACAATGTT	TCAGGCGGATCTGTTCTTCT			
Chrebpα	TTTTGACCAGATGCGAGACA	TGGCGTAGGGAGTTCAGG			
GAPDH	CAAGGAGTAAGAAACCCTGGACC	CGAGTTGGGATAGGGCCTCT			
36B4	GCTGATGGGCAAGAACACCA	CCCAAAGCCTGGAAGAAGGA			
HPRT	AGGACCTCTCGAAGTGT	TCAAATCCCTGAAGTACTCAT			

Table 1. Primer sequences and antibodies used in the present work.

Proteins from mouse liver were isolated on ice using a Tissue Protein Lysis Buffer (Invitrogen, Villebon-sur-Yvette, France) then centrifuged at 12,000 × g, 4 °C for 10 min to remove insoluble material. Protein concentration was measured with BCA reagent (Thermoscientific, Waltham, MA USA). Immuno-blot analysis was performed on gradient SDS-PAGE. The antibodies used are listed in Table 1. Protein detection and semi-quantitative analysis of western blot compared to actin were performed using iBright CL1500 imaging system (Invitrogen, Villebon-sur-Yvette, France) and the software Image J (NIH, USA), respectively. All compared samples were run on the same gel. Original blots were included in supplementary data.

Blood and tissue biochemical analysis

Frozen liver tissue (40 mg) was homogenized in 800 µl of HPLC-grade acetone. After incubation with agitation at room temperature overnight, aliquots of acetone-extract lipid suspension were used for the determination of hepatic TG content by using the kit TR0100 (Sigma-Aldrich, St louis MO, USA). Glycerol and glucose concentration were analyzed with the Free glycerol reagent F-6428 and the assay kit GAGO-20, respectively, from Sigma Aldrich. Non esterified FFA were measured with Free fatty acids, half micro test (Roche Diagnostic, Meylan, France).

Functional incorporation of radio-labelled substrate into TG

Liver was minced systematically into very small pieces and samples (200 mg) were pre-incubated in cell culture inserts (Thermoscientific, Waltham, MA USA) in multi-well plates containing glucose-free DMEM with 0.5% BSA for 2 h, then in Krebs–Henseleit bicarbonate buffer (KRBH) containing 0.5% fatty acid-free BSA, $^{14}C_1$ pyruvate (2 µCi/ml), 0.5 mM pyruvate and 1 µM (-) isoproterenol. After 2 h at 37 °C under constant agitation, the explants were rinsed in PBS, precisely weighted and frozen in liquid nitrogen before undergoing lipid extraction by the simplified method of Bligh and Dyer[52]. The incorporation of $^{14}C_1$ pyruvate into the lipid moiety was estimated by counting the radioactivity associated with this fraction. $^{14}C_1$ pyruvate was chosen because, in contrast to C_2 or C_3-labeled molecules, only the C_1 carbon of pyruvate is conserved in the G3P moiety of newly synthesized TG, and thus, is a marker for GNG. When the glycerol incorporation into TG was tested, U-^{14}C glycerol (2 µCi/ml) and 0.25 mM glycerol were added to the KRBH, and the experiment was performed without isoproterenol. Glucose incorporation was analyzed using U-^{14}C glucose (2 µCi/ml), 1 mM glucose and 100 nM insulin. When acetate was concerned, we used U-^{14}C acetate (2 µCi/ml) and 3 mM acetate.

Glucose neo-production by liver slices

Liver slices were prepared from 4 h-fasted mice as described above, then incubated in KRBH containing 0.5% BSA, 1 mM lactate and 0.1 mM pyruvate for 2 h at 37 °C with constant gentle agitation. The incubation medium was then assessed for glucose concentration.

RORα chemical ligands
SR3338 and SR1078 were respectively purchased from Cayman (Interchim, Montigny le Bretonneux, France) and from Calbiochem (Merck Chemicals, Nottingham, UK).

Statistical analysis
Values are presented as means + /− SD. Statistical analysis was performed by one-way or two-way ANOVA or by unpaired Student 's t test as mentioned in the figures caption. $p < 0.05$ was considered the limit for statistical significance.

Data availability
The authors declare that all data supporting the findings of this study are available in the article or from the corresponding author upon reasonable request.

Received: 12 August 2024; Accepted: 18 March 2025
Published online: 26 March 2025

References
1. Guan, D. & Lazar, M. A. Interconnections between circadian clocks and metabolism. *J. Clin. Investig.* **131**, e148278 (2021).
2. Ralph, M. R., Foster, R. G., Davis, F. C. & Menaker, M. Transplanted suprachiasmatic nucleus determines circadian period. *Science* **247**, 975–978 (1990).
3. Damiola, F. et al. Restricted feeding uncouples circadian oscillators in peripheral tissues from the central pacemaker in the suprachiasmatic nucleus. *Genes Dev.* **14**, 2950–2961 (2000).
4. Giguère, V. et al. Isoform-specific amino-terminal domains dictate DNA-binding properties of ROR alpha, a novel family of orphan hormone nuclear receptors. *Genes Dev.* **8**, 538–553 (1994).
5. Akashi, M. & Takumi, T. The orphan nuclear receptor RORalpha regulates circadian transcription of the mammalian core-clock Bmal1. *Nat. Struct. Mol. Biol.* **12**, 441–448 (2005).
6. Preitner, N. et al. The orphan nuclear receptor REV-ERBalpha controls circadian transcription within the positive limb of the mammalian circadian oscillator. *Cell* **110**, 251–260 (2002).
7. Marciano, D. P. et al. The therapeutic potential of nuclear receptor modulators for treatment of metabolic disorders: PPARγ, RORs, and Rev-erbs. *Cell Metab.* **19**, 193–208 (2014).
8. Lau, P. et al. The orphan nuclear receptor, RORalpha, regulates gene expression that controls lipid metabolism: Staggerer (SG/SG) mice are resistant to diet-induced obesity. *J. Biol. Chem.* **283**, 18411–18421 (2008).
9. Kang, H. S. et al. Transcriptional profiling reveals a role for RORalpha in regulating gene expression in obesity-associated inflammation and hepatic steatosis. *Physiol. Genomics* **43**, 818–828 (2011).
10. Delezie, J. et al. The nuclear receptor REV-ERBα is required for the daily balance of carbohydrate and lipid metabolism. *FASEB J. Off. Publ. Fed. Am. Soc. Exp. Biol.* **26**, 3321–3335 (2012).
11. Takeda, Y. et al. Retinoic acid-related orphan receptor γ (RORγ): A novel participant in the diurnal regulation of hepatic gluconeogenesis and insulin sensitivity. *PLoS Genet.* **10**, e1004331 (2014).
12. Lau, P., Fitzsimmons, R. L., Pearen, M. A., Watt, M. J. & Muscat, G. E. O. Homozygous staggerer (sg/sg) mice display improved insulin sensitivity and enhanced glucose uptake in skeletal muscle. *Diabetologia* **54**, 1169–1180 (2011).
13. Guastavino, J. M., Bertin, R. & Portet, R. Effects of the rearing temperature on the temporal feeding pattern of the staggerer mutant mouse. *Physiol. Behav.* **49**, 405–409 (1991).
14. Kadiri, S., Auclair, M., Capeau, J. & Antoine, B. Depot-specific response of adipose tissue to diet-induced inflammation: The retinoid-related orphan receptor α (RORα) involved?. *Obesity* **25**, 1948–1955 (2017).
15. Kadiri, S. et al. The nuclear retinoid-related orphan receptor-α regulates adipose tissue glyceroneogenesis in addition to hepatic gluconeogenesis. *Am. J Physiol. Endocrinol. Metabol.* **309**, E105–E114 (2015).
16. Lau, P. et al. Rorα deficiency and decreased adiposity are associated with induction of thermogenic gene expression in subcutaneous white adipose and brown adipose tissue. *Am. J. Physiol. Endocrinol. Metabol.* **308**, E159–E171 (2015).
17. Auclair, M., Roblot, N., Capel, E., Fève, B. & Antoine, B. Pharmacological modulation of RORα controls fat browning, adaptive thermogenesis, and body weight in mice. *Am. J. Physiol. Endocrinol. Metabol.* **320**, E219–E233 (2021).
18. Kojetin, D. J. & Burris, T. P. REV-ERB and ROR nuclear receptors as drug targets. *Nat. Rev. Drug Discovery* **13**, 197–216 (2014).
19. Kumar, N. et al. Identification of SR3335 (ML-176): A synthetic RORα selective inverse agonist. *ACS Chem. Biol.* **6**, 218–222 (2011).
20. Monnier, C., Auclair, M., Le Cam, G., Garcia, M.-P. & Antoine, B. The nuclear retinoid-related orphan receptor RORα controls circadian thermogenic programming in white fat depots. *Physiol. Rep.* **6**, e13678 (2018).
21. Molinaro, A. et al. Liver-specific RORα deletion does not affect the metabolic susceptibility to western style diet feeding. *Mol. Metabol.* **23**, 82–87 (2019).
22. Kim, K. et al. RORα controls hepatic lipid homeostasis via negative regulation of PPARγ transcriptional network. *Nat. Commun.* **8**, 162 (2017).
23. Zhang, Y. et al. The hepatic circadian clock fine-tunes the lipogenic response to feeding through RORα/γ. *Genes Dev.* **31**, 1202–1211 (2017).
24. Rudic, R. D. et al. BMAL1 and CLOCK, two essential components of the circadian clock, are involved in glucose homeostasis. *PLoS Biol.* **2**, e377 (2004).
25. Nye, C. K., Hanson, R. W. & Kalhan, S. C. Glyceroneogenesis is the dominant pathway for triglyceride glycerol synthesis in vivo in the rat. *J. Biol. Chem.* **283**, 27565–27574 (2008).
26. Udoh, U. S. et al. Genetic deletion of the circadian clock transcription factor BMAL1 and chronic alcohol consumption differentially alter hepatic glycogen in mice. *Am. J. Physiol. Gastrointest. Liver Physiol.* **314**, G431–G447 (2018).
27. Adamovich, Y. et al. Circadian clocks and feeding time regulate the oscillations and levels of hepatic triglycerides. *Cell Metab.* **19**, 319–330 (2014).
28. Sato, T. K. et al. A functional genomics strategy reveals rorα as a component of the mammalian circadian clock. *Neuron* **43**, 527–537 (2004).
29. Takeda, Y., Jothi, R., Birault, V. & Jetten, A. M. RORγ directly regulates the circadian expression of clock genes and downstream targets in vivo. *Nucleic Acids Res.* **40**, 8519–8535 (2012).
30. Delerive, P., Chin, W. W. & Suen, C. S. Identification of Reverb(alpha) as a novel ROR (alpha) target gene. *J. Biol. Chem.* **277**, 35013–35018 (2002).
31. Wang, Y. et al. A proteomics landscape of circadian clock in mouse liver. *Nat. Commun.* **9**, 1553 (2018).
32. Medvedev, A., Yan, Z. H., Hirose, T., Giguère, V. & Jetten, A. M. Cloning of a cDNA encoding the murine orphan receptor RZR/ROR gamma and characterization of its response element. *Gene* **181**, 199–206 (1996).

33. Pathak, P., Li, T. & Chiang, J. Y. Retinoic acid-related orphan receptor α regulates diurnal rhythm and fasting induction of sterol 12α-hydroxylase in bile acid synthesis. *J. Biol. Chem.* **288**, 37154–37165 (2013).
34. Liu, A. C. et al. Redundant function of REV-ERBalpha and beta and non-essential role for Bmal1 cycling in transcriptional regulation of intracellular circadian rhythms. *PLoS Genet.* **4**, e1000023 (2008).
35. Guan, D. et al. The hepatocyte clock and feeding control chronophysiology of multiple liver cell types. *Science* **369**, 1388–1394 (2020).
36. Joseph, S. B. et al. Direct and indirect mechanisms for regulation of fatty acid synthase gene expression by liver X receptors. *J. Biol. Chem.* **277**, 11019–11025 (2002).
37. Kim, E.-J. et al. Retinoic acid receptor-related orphan receptor α-induced activation of adenosine monophosphate-activated protein kinase results in attenuation of hepatic steatosis. *Hepatology* **55**, 1379–1388 (2012).
38. Takeda, Y. et al. Retinoid acid-related orphan receptor γ, RORγ, participates in diurnal transcriptional regulation of lipid metabolic genes. *Nucleic Acids Res.* **42**, 10448–10459 (2014).
39. Yoshikawa, T. et al. Identification of liver X receptor-retinoid X receptor as an activator of the sterol regulatory element-binding protein 1c gene promoter. *Mol. Cell. Biol.* **21**, 2991–3000 (2001).
40. Matsumoto, E. et al. Time of day and nutrients in feeding govern daily expression rhythms of the gene for sterol regulatory element-binding protein (SREBP)-1 in the mouse liver. *J. Biol. Chem.* **285**, 33028–33036 (2010).
41. Gilardi, F. et al. Genome-wide analysis of SREBP1 activity around the clock reveals its combined dependency on nutrient and circadian signals. *PLoS Genet.* **10**, e1004155 (2014).
42. Yabe, D., Komuro, R., Liang, G., Goldstein, J. L. & Brown, M. S. Liver-specific mRNA for Insig-2 down-regulated by insulin: Implications for fatty acid synthesis. *Proc. Natl. Acad. Sci. USA.* **100**, 3155–3160 (2003).
43. Cervino, A. C. et al. Integrating QTL and high-density SNP analyses in mice to identify Insig2 as a susceptibility gene for plasma cholesterol levels. *Genomics* **86**, 505–517 (2005).
44. Yang, T. et al. crucial step in cholesterol homeostasis. *Cell* **110**, 489–500 (2002).
45. Le Martelot, G. et al. REV-ERBalpha participates in circadian SREBP signaling and bile acid homeostasis. *PLoS Biol.* **7**, e1000181 (2009).
46. Dyar, K. A. et al. Atlas of circadian metabolism reveals system-wide coordination and communication between clocks. *Cell* **174**, 1571-1585.e11 (2018).
47. Hunter, A. L. et al. Nuclear receptor REVERBα is a state-dependent regulator of liver energy metabolism. *Proc. Natl. Acad. Sci. USA.* **117**, 25869–25879 (2020).
48. Slominski, A. T. et al. RORα and ROR γ are expressed in human skin and serve as receptors for endogenously produced noncalcemic 20-hydroxy- and 20,23-dihydroxyvitamin D. *FASEB J* **28**, 2775–2789 (2014).
49. Slominski, A. T. et al. Endogenously produced nonclassical vitamin D hydroxy-metabolites act as "biased" agonists on VDR and inverse agonists on RORa and RORg. *J. Steroid. Biochem. Mol. Biol.* **173**, 42–56 (2017).
50. He, B. et al. The small molecule Nobiletin targets the molecular oscillator to enhance circadian rhythms and protect against metabolic syndrome. *Cell metab.* **23**, 610–621 (2016).
51. Han, Y. H. et al. RORα Induces KLF4-mediated M2 polarization in the liver macrophages that protect against nonalcoholic steatohepatitis. *Cell Rep* **5**, 124–135 (2017).
52. Bligh, E. G. & Dyer, W. J. A rapid method of total lipid extraction and purification. *Can. J. Biochem. Physiol.* **37**, 911–917 (1959).

Acknowledgements

We greatly thank Tatiana Ledent and Laetitia Dinard for their help in the sg/sg mice-housing facility. B.A. is a CNRS researcher.

Author contributions

Conceptualization: B.A.; Methodology: C.M., M.G., M.A., N.R., A.B.B., P.K.B. and B.A.; Validation: C.M., M.G., M.A., N.R., A.B.B., P.K.B., B.F. and B.A.; Formal analysis: C.M., M.G., B.F. and B.A.; Resources: B.F. and B.A.; Writing-original draft preparation: C.M., B.F. and B.A.; Visualization: C.M., M.G., M.A., N.R., A.B.B., P.K.B., B.F. and B.A; Supervision: B.F.; Project administration: B.A.

Funding

Our funding is from CNRS, Inserm, Sorbonne University and "la Fondation pour la Recherche Médicale" (EQU201903007868).

Declarations

Competing interests

The authors state that they have no competing interests.

Additional information

Supplementary Information The online version contains supplementary material available at https://doi.org/10.1038/s41598-025-95228-y.

Correspondence and requests for materials should be addressed to B.A.